PHYSICAL REVIEW C, VOLUME 65, 041302(R)

Giant halo at the neutron drip line in Ca isotopes in relativistic continuum Hartree-Bogoliubov theory

J. Meng,[1,2,3,4,*] H. Toki,[2] J. Y. Zeng,[1,3,4] S. Q. Zhang,[1] and S.-G. Zhou[1,3,4]
[1]*School of Physics, Peking University, Beijing 100871 People's Republic of China*
[2]*Research Center for Nuclear Physics, Osaka University, Ibaraki 567-0047, Japan*
[3]*Institute of Theoretical Physics, Chinese Academy of Science, Beijing 100080 People's Republic of China*
[4]*Center of Theoretical Nuclear Physics, National Laboratory of Heavy Ion Accelerator, Lanzhou 730000 People's Republic of China*
(Received 28 November 2001; published 11 March 2002)

The properties of even-even O, Ca, Ni, Zr, Sn, and Pb isotopes from the β-stability line to the neutron drip line are studied with the relativistic continuum Hartree-Bogoliubov theory, where both the spin-orbit interaction and continuum are properly taken into account. The available experimental binding energies E_b and two-neutron separation energies S_{2n} are reproduced very well. The predicted neutron drip-line nuclei are, respectively, ^{74}Ca, ^{100}Ni, ^{140}Zr, ^{176}Sn, and ^{268}Pb. Based on the analysis of two-neutron separation energies, single-particle energy levels, the orbital occupation, the contribution of continuum and nucleon density distribution, giant halo phenomena due to pairing, correlation and the contribution from the continuum are suggested to appear in Ca isotopes with $A>60$ apart from Zr isotopes predicted earlier.

DOI: 10.1103/PhysRevC.65.041302 PACS number(s): 21.10.Gv, 21.60.Jz, 27.40.+z

The study of exotic nuclei far away from the line of β stability has attracted world wide attention [1,2]. Unexpected properties very different from that of normal nuclei have been observed in light nuclei, such as, for instance, the neutron halo in ^{11}Li [3]. They consist of a normal core surrounded by a layer of low-density neutron matter, i.e., halo or skin. However, in all of the halos observed so far, one has only one or two particles outside of the normal core.

Theoretically, it has been shown in Ref. [4] that the formation of a neutron halo can be understood as the scattering of Cooper pairs into the continuum containing low-lying resonances of small angular momentum based on the relativistic continuum Hartree-Bogoliubov (RCHB) theory [5]. The advantages of the RCHB theory include the following: Being relativistic it is able to take into account the proper isospin dependence of the spin-orbit term and at the same time a reliable description of nuclei far away from the β-stability line. In addition this theory provides a self-consistent treatment of pairing correlations in the presence of the continuum. The halo phenomena can be understood in this self-consistent picture as the scattering of particle pairs into the continuum by the pairing force. Along this line a new phenomenon—giant neutron halos—has been also predicted in the Zr nuclei close to the neutron drip line [6]. They are formed by two to six neutrons scattered as Cooper pairs mainly to the levels $3p_{3/2}$, $2f_{7/2}$, $3p_{1/2}$, and $2f_{5/2}$.

Since its suggestion, the giant halo has attracted lots of interest from the experimental side. However, due to the limit of the experimental facilities it has not been observed so far. Even for the new RIB factory under construction now in RIKEN, the intensity of RIB is not strong enough to produce these beams for the discovery of giant halos except for the beginning of halos in Zr [7]. It will be very exciting and challenging both theoretically and experimentally to explore new regions of giant halos, particularly in relatively light nuclei so that the present and the planned facilities can reach these nuclei.

In this paper we report on the theoretical exploration of neutron halos and giant halos for proton magic isotopes close to the neutron drip line in the on-line mass region.

The detailed formalism and numerical techniques of the RCHB theory can be found in Ref. [5], and references therein. In the relativistic mean field theory, one describes the nucleons with the mass m as Dirac spinors ψ moving in the fields of mesons: a isoscalar-scalar meson (σ), an isoscalar-vector meson (ω), an isovector-vector meson ($\vec{\rho}$) and the photon A^μ, with the masses m_σ, m_ω, and m_ρ and the coupling constants g_σ, g_ω, and g_ρ. The field tensors for the vector mesons are given as $\Omega_{\mu\nu}=\partial_\mu\omega_\nu-\partial_\nu\omega_\mu$ and by similar expressions for the ρ meson and the photon, i.e.,

$$\begin{aligned}\mathcal{L}=&\bar{\psi}(\not{p}-g_\omega\not{\omega}-g_\rho\not{\vec{\rho}}\vec{\tau}-\tfrac{1}{2}e(1-\tau_3)\not{A}-g_\sigma\sigma-m)\psi\\&+\tfrac{1}{2}\partial_\mu\sigma\partial^\mu\sigma-U_1(\sigma)-\tfrac{1}{4}\Omega_{\mu\nu}\Omega^{\mu\nu}+U_2(\omega)\\&-\tfrac{1}{4}\vec{R}_{\mu\nu}\vec{R}^{\mu\nu}+\tfrac{1}{2}m_\rho^2\vec{\rho}_\mu\vec{\rho}^\mu-\tfrac{1}{4}F_{\mu\nu}F^{\mu\nu}.\end{aligned}\tag{1}$$

The nonlinear self-coupling terms, $U_1(\sigma)=\frac{1}{2}m_\sigma^2\sigma^2+\frac{1}{3}g_2\sigma^3+\frac{1}{4}g_3\sigma^4$ for the σ mesons, and $U_2(\omega)=\frac{1}{2}m_\omega^2\omega_\mu\omega^\mu+\frac{1}{4}c_3(\omega_\mu\omega^\mu)^2$ for the ω mesons, have been included as well.

From the above Lagrangian one can derive the relativistic Hartree-Bogoliubov (RHB) equations; for the details see Ref. [8]. In the pairing channel a density dependent two-body force of zero range has been used instead of the one-meson exchange interaction, just as that in Refs. [4,5].

In order to describe the continuum and its coupling to the bound states properly, the RHB equation must be solved in coordinate space and extended to include the contribution of the continuum, i.e., the RCHB theory [5]. We restricted our study to the proton magic nuclei, so that we can impose the

*Email address: mengj@pku.edu.cn

spherical symmetry. For zero range pairing forces the relativistic Hartree Bogoliubov (HB) equations are a set of four coupled differential equations for the HB Dirac spinors $U(r)$ and $V(r)$.

The detailed formalism and numerical techniques can be found in Ref. [5]. In the present calculations, we follow the procedures in Refs. [5,9] and solve the RCHB equations in a box with the size $R=20$ fm and a step size of 0.1 fm. The parameter set NL-SH [10] is used, which aims at describing both the stable and exotic nuclei. The use of other parameters such as $TM1$ does not provide very different results [11]. The contribution from continua is restricted within a cutoff energy $E_{cut}\sim 120$ MeV. For fixed cut-off energy and for fixed box radius R the strength V_0 of the pairing force is determined by adjusting the corresponding pairing energy $-\frac{1}{2}\mathrm{Tr}\Delta\kappa$ to that of a RCHB calculation using the finite range part of the Gogny force $D1S$, as in Ref. [5]. For ρ_0 in the pairing force we use the nuclear matter density 0.152 fm^{-3}.

All the even-even Ca nuclei ranging from proton drip line to neutron drip line, as well as other proton magic nuclei, e.g., O, Ni [5], Zr [6], Sn [12], and Pb isotope chains are studied with the RCHB code. The last bound neutron-rich nucleus for Ca is predicted as ^{72}Ca, while in Ref. [13] and Refs. [14,15], the drip-line nucleus is predicted as ^{72}Ca with the Hartree-Fock-Bogoliubov and Skyrme Hartree-Fock (HF) method, respectively. The Skyrme HF results with $SIII$ and SkM^* show that $^{60-70}$Ca is bound due to the last bound orbit $1g_{9/2}$ [15]. In RCHB, as in the following, it is shown that these nuclei are bound due to different mechanisms. The orbits $1g_{9/2}$ and $3s_{1/2}$ are in the continuum. Without pairing, the nuclei $^{60-72}$Ca are unbound. After taking into account the pairing, the contribution from the continuum is switched on, then we get the bound $^{60-72}$Ca. As their two-neutron separation energies are due to the pairing and are very small, the giant halo phenomena develop in these nuclei. In addition, the proton drip-line nucleus is predicted to be ^{34}Ca, which has been discovered in radioactive ion beam experiments. The binding energy E_b calculated from the RCHB for Ca isotopes reproduce the available data well [16]. The difference between the experimental and calculated binding energies is less than 3 MeV.

The two-neutron separation energy S_{2n} is quite a sensitive quantity to test a microscopic theory. Both the theoretical and the available experimental S_{2n} for O, Ca, Ni, Zr, Sn, and Pb isotopes are presented in Fig. 1. The good agreement between experiment and calculation is clearly shown. For the light isotope as O, we find that the RCHB calculations provide the drip-line nucleus to be ^{30}O, while experimentally it is known as ^{26}O. It is known that in relativistic mean field, one parameter set is used to describe all nuclei in the nuclear chart. This is very challenging. Particularly, as it is well known, the mean field theory is difficult for light nuclei. Therefore we have NL1, NLSH, NL3, and TM1 for the heavy system and NL2 and TM2 for the light system. The oxygen isotopes lie just near the border line. It is not surprising that the NLSH, NL1, NL2, NL3, TM1, TM2 and the nonrelativistic counterparts do not predict the correct neutron drip line which is already known experimentally to be at ^{26}O.

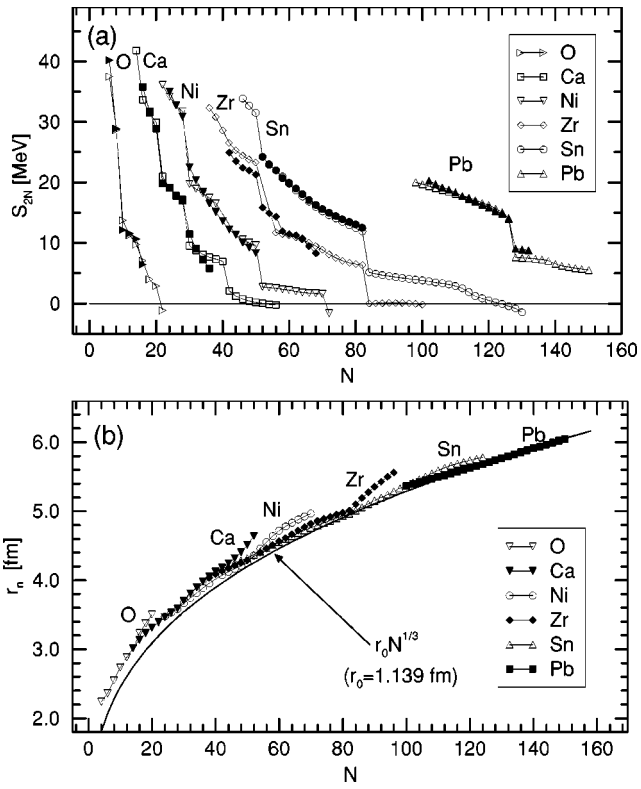

FIG. 1. (a) The two-neutron separation energies S_{2n} in even Ca, Ni, Zr, Sn, and Pb isotopes are plotted against the neutron number N. Open symbols represent the values calculated from the RCHB theory with the NLSH parameter set while solid ones represent the data available. (b) The root mean square neutron radius r_n for even Ca, Ni, Zr, Sn and Pb isotopes from RCHB calculation as a function of the neutron number N. The curve for the $r_0N^{1/3}$ rule with $r_0=1.139$ fm has been included to guide the eye.

Along the S_{2n} versus N curve for Ca isotopes, three strong kinks appear at the magic or submagic numbers $N=20$, 28, and 40, respectively. However, there seems no kink at the other magic number $N=50$, which suggests the disappearance of the neutron magic number $N=50$. Therefore the nucleus ^{70}Ca is no more a double-magic nucleus. This disappearance of the $N=50$ magic number at the neutron drip line is due to the halo property of the neutron density with the spherical shape being kept, which is different from the disappearance of the $N=20$ magic number due to deformation. Most recently a new magic number $N=16$ has been discovered in neutron drip-line light-nuclei region [17]. All these suggest that the single-particle level energies and their orders will vary violently in the near drip-line region, then result in the change of the traditional magic numbers. We do not observe the so-called two-neutron drip-line double-magic emitter predicted in Ref. [13], i.e., ^{70}Ca comes out with $\Delta=0$ and the calculated S_{2n} value is negative, -236 keV.

Another remarkable appearance in Fig. 1 is that the S_{2n} values for exotic Ca isotopes are extremely close to zero in several isotopes, i.e., $S_{2n}\approx 2.06$ MeV for ^{62}Ca, 1.24 MeV

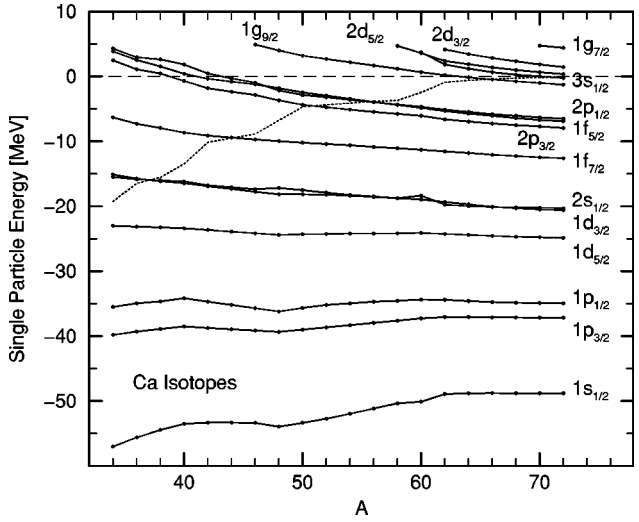

FIG. 2. The neutron single-particle levels in the canonical basis with the mass number A for Ca isotopes. The Fermi surface is shown as the dotted line.

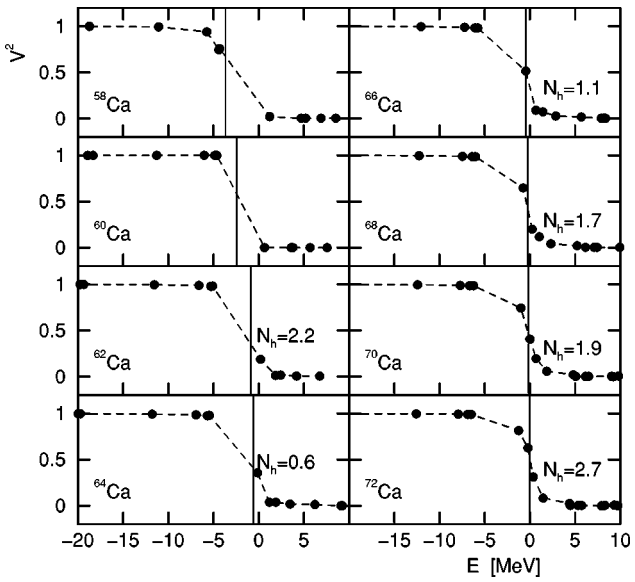

FIG. 3. The occupation probabilities in the canonical basis for several Ca isotopes as a function of the single-particle energy. The chemical potential is indicated by a vertical line. The numbers N_h of neutrons in the continuum are also shown.

for ^{64}Ca, 0.76 MeV for ^{66}Ca, 0.53 MeV for ^{68}Ca, 0.21 MeV for ^{70}Ca, and 0.04 MeV for ^{72}Ca. If one regards ^{60}Ca as a core, then the valence neutrons are filled in the weakly bound levels and continuum above the $N=40$ subshell for these nuclei, especially for $^{66-72}$Ca. This is very similar to S_{2n} in Zr isotopes with $N>82$ [6]. However in the vicinity of the drip line, S_{2n} in Sn [12] decrease rather rapidly with the mass number A and that in Ni [5] are quite large ($\sim$2 MeV) with a sudden drop at the drip-line nucleus. All such results can be well understood with the single particle energy levels in the threshold region, as shown in Ref. [12]. It should be noted that the behavior of S_{2n} indicates the appearance of a "*giant halo*" in Ca chains, just as that in Zr chains [6].

To illustrate the probable "*giant halo*," the calculated neutron radii r_n from the RCHB calculation for even-even nuclei in O, Ca, Ni, Zr, Sn, and Pb isotopes are plotted in Fig. 1. It is very interesting to see that r_n follow the $N^{1/3}$ systematics well for stable nuclei although their proton number is quite different. Near the drip line, abnormal behaviors appear at $N=40$ in Ca isotopes and at $N=82$ in Zr isotopes. The increase of r_n in exotic Ni and Sn nuclei is not as fast as that in Ca and Zr. The nuclei at the abnormal r_n increase correspond to those for S_{2n}. They give further support for the formation of a *giant halo*. Compared with Zr isotopes, the *giant halo* in Ca isotopes will be easy to access experimentally. Of course there are also some abnormal changes for the Ni and Sn isotopes near the neutron drip line, but they are not as obvious as the Ca and Zr cases.

To understand the above results more clearly, we will see the microscopic structure of the single-particle spectrum in the canonical basis [5]. In Fig. 2, the neutron single-particle levels in the canonical basis are shown for the even Ca isotopes from the mass numbers $A=34$ to $A=72$. The shell closure ($N=20,28$) and subshell closure ($N=40$) are clearly seen as big gaps between levels. A dotted line in the figure represents the neutron chemical potential λ_n, which jumps three times at the magic or submagic neutron number on its way to the drip-line nucleus ^{74}Ca and comes close to zero ($<1s$ MeV) when $A>60$. As mentioned above, similar kinks appear in the S_{2n} case. These jumps correspond to the shell (or subshell) closure. Meanwhile, another traditional magic number $N=50$, which is due to a big gap between the $1g_{9/2}$ orbit and its above s-d shell, has disappeared here. Therefore there is no kink at $N=50$ in the λ_n curve due to the lowering of $3s_{1/2}$ and $2d_{5/2}$ orbits.

As the chemical potential λ approaches zero, the Ca isotopes with $A>60$ are all weakly bound. This means that the additional neutrons occupy either weakly bound states or the continuum. They supply very small binding energy. As the Fermi level is so close to zero, pairing correlations will scatter the neutron pairs from bound states to continua. For Ca isotopes with $A>60$, the last neutrons filled in the continuum and weakly bound levels in the gross order: $1g_{9/2}$, $3s_{1/2}$, $2d_{5/2}$, $2d_{3/2}$, etc. Such orbits will take on an important role as discussed below.

In Fig. 3 the occupation probabilities v^2 of neutron levels near the Fermi surface (i.e., $-20\leqslant E\leqslant 10$ MeV) in the canonical basis are shown for several neutron-rich even Ca isotopes. The chemical potential is indicated by a vertical line. For nuclei near the β-stability line, the chemical potential is about 7 MeV, and the occupation probability for the continuum ($E>0$) is nearly zero. As the neutron number goes beyond the subshell $N=40$, the Fermi surface will move to zero and the occupation of the continuum becomes more and more important. Adding up the occupation probabilities v^2 for the levels with $E>0$, one can get the contribution of the continuum n_h [6]. They are approximately 2.2, 0.6, 1.1, 1.7, 1.9, and 2.7 for ^{62}Ca, ^{64}Ca, ^{66}Ca, ^{68}Ca, ^{70}Ca, and ^{72}Ca, respectively.

As a typical example, the neutron single-particle levels in ^{66}Ca in the canonical basis are given in Fig. 4. The length of

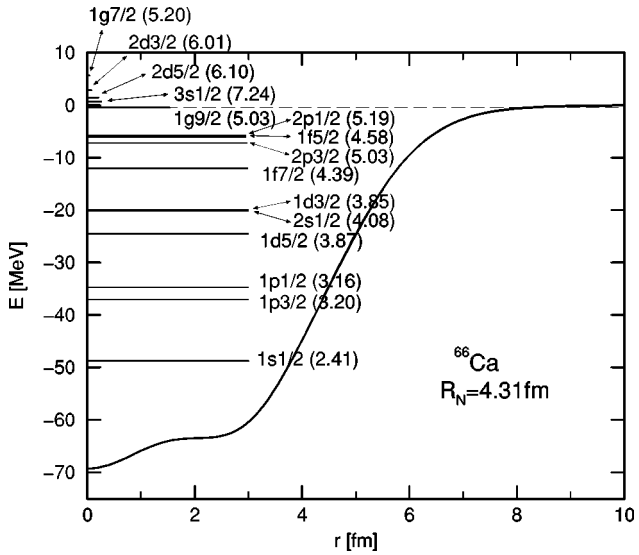

FIG. 4. The neutron single-particle levels in the canonical basis in ^{66}Ca. The neutron potential $V(r)+S(r)$ is represented by the solid curve and the Fermi surface is shown as a dashed line. The occupation probabilities for the single-particle levels are proportional to their length. The root mean square radius r_{nlj} for each orbit is shown in fertometers in the parentheses behind the corresponding labels.

each level is proportional to its occupation. The root mean square radius r_{nlj} in fentometers for each level is shown in the parentheses behind the corresponding label. The root mean square radius r_{nlj} is defined as $r_{nlj}=(\int\rho_{nlj}r^2d\tau)/(\int\rho_{nlj}d\tau)$. The nuclear mean field potential $V(r)+S(r)$ is shown by the solid curve. The Fermi surface $\lambda_n\approx-0.435$ MeV for neutrons is given as a dashed line. The state $1g_{9/2}$ is weakly bound with the energy -0.48 MeV, while the $3s_{1/2}$, $2d_{5/2}$, $2d_{3/2}$, and $1_{g7/2}$ levels are in the continuum with energies 0.64, 1.41, 2.85, and 5.67 MeV, respectively. Due to the absence of a centrifugal barrier, the orbit $3s_{1/2}$ lies below states $2d_{3/2}$, $2d_{5/2}$, and $1g_{7/2}$. The occupation probabilities v^2 of these states are, respectively, 0.514 for $1g_{9/2}$, 0.089 for $3s_{1/2}$, 0.071 for $2d_{5/2}$, 0.027 for $2d_{3/2}$, and 0.017 for $1g_{7/2}$. There are about 0.86 neutrons in the continuum. The state $3s_{1/2}$ has a rms radius 7.24 fm in comparison with the rms radii of the neighbor states ($\sim$5 fm) and the total neutron (4.314 fm) due to the zero centrifugal barrier. Therefore the nucleon occupying the state $3s_{1/2}$ will contribute to the nuclear rms radius considerably. That is the main reason why the neutron radii of exotic Ca isotopes present the abnormal rapid increase in neutron number near the drip line.

In summary, the ground state properties of even-even O, Ca, Ni, Zr, Sn, and Pb isotopes from β stability to the neutron drip-line have been investigated with the self-consistent relativistic continuum Hartree-Bogoliubov theory. The binding energies, two-neutron separation energy S_{2n}, and rms radii are calculated and compared with the data available. Satisfactory agreement with the data available has been observed. The predicted neutron drip-line nuclei are, respectively, ^{74}Ca, ^{100}Ni, ^{140}Zr, ^{176}Sn, and ^{268}Pb. It is interesting to note that the drip line nucleus for Ca is $N=54$, not $N=50$, due to the disappearance of the $N=50$ magic shell. Based on the analysis of two-neutron separation energies S_{2n}, rms radii, single-particle levels spectra, the orbital occupation, and the contribution of the continuum, giant halo phenomena are suggested to appear in Ca isotopes with $A>60$ apart from Zr isotopes predicted earlier. This will be found relatively easily by experiment. Without pairing, the nuclei $^{60-72}$Ca will be unbound as the $1g_{9/2}$ and $3s_{1/2}$ are in the continuum. After taking into account the pairing, the contribution from the continuum is switched on, and then we get the bound $^{60-72}$Ca. As their two-neutron separation energies are mainly due to the pairing and they are very small, the giant halo phenomena develop in these nuclei.

This work was partly supported by the Major State Basic Research Development Program Under Contract No. G2000077407 and the National Natural Science Foundation of China under Grant Nos. 10025522, 19847002, and 19935030. J.M. would like to thank the Research Center for Nuclear Physics in Osaka University for its hospitality and the COE program of the Ministry of Education, Science, and Technology for its support.

[1] I. Tanihata, Prog. Part. Nucl. Phys. **35**, 505 (1995).
[2] A.C. Müller, Prog. Part. Nucl. Phys. **46**, 359 (2001).
[3] I. Tanihata *et al.*, Phys. Rev. Lett. **55**, 2676 (1985).
[4] J. Meng and P. Ring, Phys. Rev. Lett. **77**, 3963 (1996)
[5] J. Meng, Nucl. Phys. **A635**, 3 (1998).
[6] J. Meng and P. Ring, Phys. Rev. Lett. **80**, 460 (1998).
[7] I. Tanihata, Nucl. Phys. **A685**, 80c (2001).
[8] H. Kucharek and P. Ring, Z. Phys. A **339**, 23 (1991).
[9] J. Meng, I. Tanihata, and S. Yamaji, Phys. Lett. B **419**, 1 (1998).
[10] M.M. Sharma, M.A. Nagarajan, and P. Ring, Phys. Lett. B **312**, 377 (1993).
[11] Y. Sugahara and H. Toki, Nucl. Phys. **A579**, 557 (1994).
[12] J. Meng and I. Tanihata, Nucl. Phys. **A650**, 176 (1999).
[13] S.A. Fayans, S.V. Tolokonnikov, and D. Zawischa, Phys. Lett. B **491**, 245 (2000).
[14] Soojae Im and J. Meng, Phys. Rev. C **61**, 047302 (2000).
[15] I. Hamamoto, H. Sagawa, and X.Z. Zhang, Phys. Rev. C **64**, 024313 (2001).
[16] G. Audi and A.H. Wapstra, Nucl. Phys. **A565**, 1 (1993).
[17] A. Ozawa, T. Kobayashi, T. Suzuki, K. Yoshida, and I. Tanihata, Phys. Rev. Lett. **84**, 5493 (2000).